Photophysics of GaSe/InSe Nanoparticle Heterojunctions†

Xiang-Bai Chen and David F. Kelley*

Division of Natural Sciences, University of California at Merced, Merced, California 95344

Received: July 14, 2006; In Final Form: August 31, 2006

The photophysics of mixed aggregates of GaSe/InSe nanoparticles have been studied using static and time-resolved absorption and emission spectroscopies. The results indicate that the GaSe/InSe interfaces form heterojunctions and exhibit photoinduced direct charge transfer from the GaSe valence band to the InSe conduction band. This results in the electrons and holes being localized separately in these two types of nanoparticles. The energy diagram of the nanoparticle heterojunction can be constructed from the static spectra, known bulk band offsets, and quantum confinement effects. These considerations accurately predict the energy of the observed charge-transfer band. Photoexcitation also produces excitons in the aggregates, away from the heterojunctions. These excitons can undergo diffusion and quench upon reaching a heterojunction. Time-resolved fluorescence kinetics can be modeled to extract an exciton diffusion coefficient. A value of 2.0 nm^2/ns is obtained, which is in good agreement with values obtained from previous fluorescence anisotropy decay measurements.

Introduction

GaSe and InSe are two-dimensional layered materials consisting of strongly covalently bonded Se−Ga−Ga−Se or Se−In−In−Se tetralayer sheets. The sheets are attached to each other by weak van der Waals interactions, making the material highly anisotropic. GaSe and InSe have the same crystal structure with similar lattice constants and similar electronic structures. Both form disklike nanoparticles consisting of single tetralayer sheets.[1,2] The spectroscopy of these nanoparticles can be understood in terms of the spectroscopy of the bulk materials and quantum confinement effects. The electronic band structures of both GaSe and InSe have been qualitatively understood for some time[3−5] and have recently been calculated in tight-binding approximation.[6] Bulk GaSe is an indirect band gap semiconductor with a band gap of ∼2.05 eV. The top of the valence band is at Γ, and the bottom of the conduction band is at M. The Γ-point in the conduction band is very slightly higher in energy, 25 meV. The lowest allowed transition ($\Gamma_4^- \rightarrow \Gamma_3^+$) is polarized along the *z*-axis. The Γ_5^-, Γ_5^+, Γ_6^-, and Γ_6^+ states are slightly deeper in the valence band, and the much more intense $\Gamma_6^- \rightarrow \Gamma_3^+$ transition is polarized in the *xy*-plane. Unlike GaSe, InSe is a direct band gap material at Γ, with the M point in conduction at a slightly higher energy. In both GaSe and InSe nanoparticles, quantum confinement effects involve energies that are much larger than the Γ−M conduction band energy separation in bulk materials, and the lowest point of the conduction band (Γ or M) is particle-size-dependent in both cases.[7,8]

Both GaSe and InSe nanoparticles stack to form strongly interacting one-dimensional aggregates.[9,10] The reason that the aggregates of these nanoparticles interact much more strongly than other types of semiconductor nanoparticles is their morphology; their two-dimensional structure allows the particle centers to get very close to each other. In this case, photoexcitation produces a delocalized exciton that is analogous to excitons in J-aggregates of organic dyes. These excitons can migrate or diffuse along the one-dimensional aggregate.[10] The similarity of GaSe and InSe nanoparticles suggests that mixed aggregates would spontaneously form in concentrated solutions or upon precipitation onto surfaces. The presence of strong interparticle interactions in mixed aggregates opens up the possibility of facile charge transfer. In a preliminary report, we showed that such mixed aggregates could be formed and that interparticle interactions result in a heterojunction charge-transfer band in the absorption spectrum.[11]

One important issue in these semiconductor heterojunctions is the band alignment, which to a large extent determines the optoelectronic properties of the heterojunction. Band alignment of GaSe/InSe thin film heterojunctions has been measured using photoelectron spectroscopy and can be understood in terms of the electron affinity rule.[12] The spectra show that the GaSe valence band edge is slightly above that of the InSe. In the case of GaSe/InSe nanoparticle heterojunctions, it should be possible to control the band alignments by controlling the particle sizes, i.e., through quantum confinement effects. In a previous paper, we showed that a InSe → GaSe charge-transfer band occurred in InSe/GaSe (10:1) mixed aggregates.[11] Those studies involved small, strongly quantum-confined particles, 2.9 nm InSe particles and 2.7 nm GaSe particles. From these results, a qualitative picture of the band alignments involving strongly quantum-confined InSe and GaSe nanoparticles could be derived. At first sight, these energetic results appeared very different than those derived on bulk thin films. However, the role of quantum confinement in the energetics of these heterojunctions was not analyzed in detail. In this paper we continue the study of InSe/GaSe heterojunctions. We report the spectroscopy and dynamics of GaSe/InSe (10:1) aggregates involving large (10 nm) GaSe particles and 3 nm InSe particles. The results are analyzed in terms of simple quantum confinement theory and the band alignments in bulk thin film heterojunctions. These results are compared to those obtained in the previous study.

The exciton diffusion dynamics in chromophore aggregates are crucial to long-range energy transport. In the case of mixed

† Part of the special issue "Arthur J. Nozik Festschrift".

* Author to whom correspondence should be addressed. E-mail: dfkelley@ucmerced.edu.

10.1021/jp064477u CCC: $33.50
Published on Web 09/30/2006

GaSe/InSe nanoparticle aggregates, exciton diffusion to a heterojunction may be followed by charge separation. We therefore also analyze the exciton diffusion dynamics in the mixed aggregates.

Experimental Section

Synthesis. The GaSe nanoparticles were prepared by a method similar to that used in previous publications.[1,10] Initially, Se (0.3925 g) and trioctylphosphine (TOP) (8.9 mL) are added into a flask, and 0.7 mL of $GaMe_3$/TOP solution is injected at room temperature. The TOP used in these syntheses was purified by vacuum distillation, extraction with dried and distilled methanol, and finally another vacuum distillation. It is then stored under dry nitrogen. We suspect that small amounts of other binding ligands (impurities) could be present in the raw or even singly vacuum distilled TOP and can effect the energetics of the particles. TOP purified by the above procedure should be quite free of such impurities. The solution is heated under nitrogen to 280 °C in ~13 min, then cooled to 268 °C and kept at this temperature for 90 min. The reaction mixture is rapidly cooled to ~50−80 °C. Subsequently, 0.63 mL aliquots of the TOP/Se and $GaMe_3$/TOP solutions are added to the reaction flask. The solution of TOP/Se is made from 6.0 mL of purified TOP with 0.7110 g of Se (99.999%), and the solution of $GaMe_3$/TOP is made by mixing 1.02 mL of $GaMe_3$ with 6.0 mL of purified TOP. The reaction mixture is then reheated to 268 °C, kept at that temperature for 90 min, and then cooled again to 50−80 °C. A small amount of precipitate appears, so the sample is then transferred under nitrogen to a centrifuge tube and centrifuged for 5 min. The supernatant is injected into a clean flask, and then additional 0.63 mL aliquots of the TOP/Se and $GaMe_3$/TOP solutions are added. The reaction mixture is then reheated to 268 °C, allowed to react for 90 min, and then cooled again to 50−80 °C. The centrifugation−add−heat−cool cycle is repeated two more times, with injections of 1.25 mL of each of the TOP/Se and $GaMe_3$/TOP solutions. The absorption of the final solution is measured, as shown in Figure 1A. The approximate absorption onset is determined from the figure to be ~469 nm, which indicates that the GaSe particles have diameters of ~10 nm.[13]

The InSe nanoparticles used in this study are synthesized using a method similar to that reported earlier.[2] Se (0.36 g), purified TOP (6 mL), and vacuum distilled trioctylphosphine oxide (TOPO) (0.5 g) are added to a flask under an argon atmosphere. The mixture is then stirred at 188 °C for 2.5 h. The solution is then heated to 288 °C, and 5 mL of trimethylindium in TOP (approximately 1 M) is injected. Upon injection, the temperature drops to 206 °C, and then the solution is reheated to 278 °C for particle growth. When the temperature reaches the target temperature, the solution turns yellow, and 2−3 min after the temperature reaches 278 °C, the solution turns dark red. The solution is then cooled rapidly to room temperature. At this point, the largest particles precipitate, and the solution turns yellow. Absorption of the top clear solution is measured and is shown in Figure 1A. The approximate absorption onset is 463 nm, and these particles are very similar to the small (~3 nm) InSe nanoparticles previously reported.[2] The GaSe/InSe mixture was prepared using 0.13 mL of GaSe and 0.07 mL of InSe diluted in 2 mL of dry, distilled octane. Thus, the final solution is approximately 90% octane, 9.7% TOP, and 0.3% TOPO. The GaSe and InSe volumes are selected so that the absorbance at 387.5 nm associated with the absorption of GaSe is 10 times of that of the InSe particles. In the strong quantum confinement limit, the lowest exciton absorption cross-section is expected to be approximately independent of particle size.[14,15] These spectra are shown in Figure 1B. Thus, despite the differences in particle sizes, this absorbance ratio approximately corresponds to a 10:1 particle number ratio.

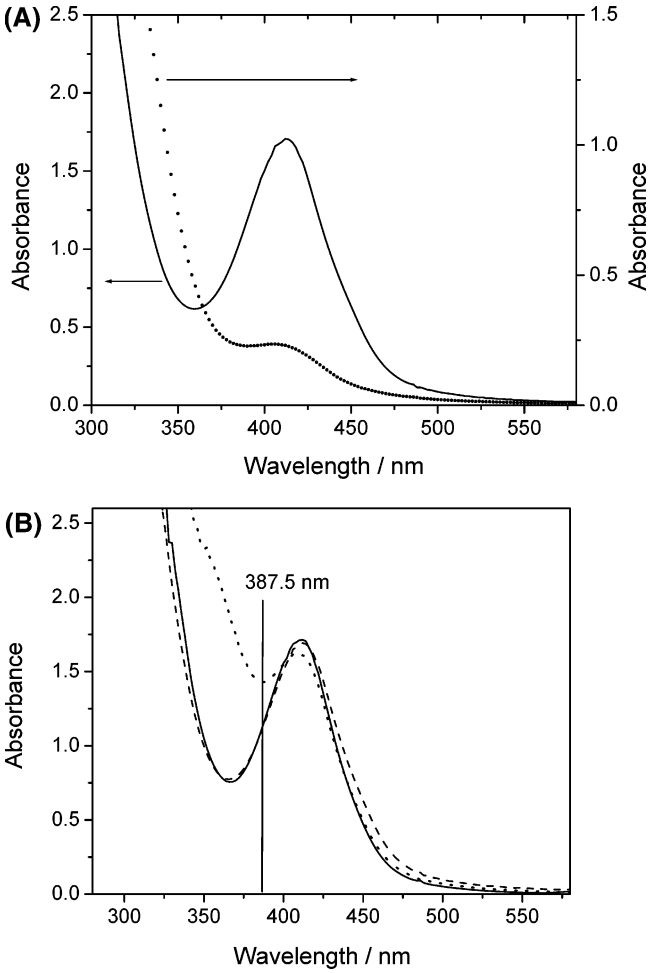

Figure 1. Static absorption spectra of (A) GaSe nanoparticles (solid curve) and InSe nanoparticles (dotted curve) and (B) GaSe/InSe nanoparticles upon mixing (solid curve) and at equilibrium (dotted curve). Also, a calculated spectrum from GaSe and InSe contributions is shown (dashed curve).

Optical Measurements. Static absorption spectra were obtained using a HP 8452A diode array spectrophotometer. Transient absorption (TA) measurements were made using the femtosecond absorption spectrometer described previously.[10] The samples are excited with linearly polarized 387.5 nm light and probed in the 475−750 nm spectral range. Static fluorescence spectra were measured on a Spex-Fluorolog-3 system. Time-resolved emission data were obtained using a time-correlated single photon counting apparatus with emission collected in a near-collinear geometry. The excitation wavelength in both static emission and time-resolved emission was chosen to be the same as that in the transient absorption experiments, 387.5 nm.

Results and Discussion

Static Spectral Assignments. The static absorption spectra of the GaSe particles, the InSe particles, and the GaSe/InSe mixture are shown in Figure 1. The spectrum of the mixture is measured upon mixing and 1 day later (Figure 1B). The absorption spectrum measured upon mixing is found to match the spectrum calculated from the GaSe and InSe contributions. The sample evolves over the course of several hours and reaches

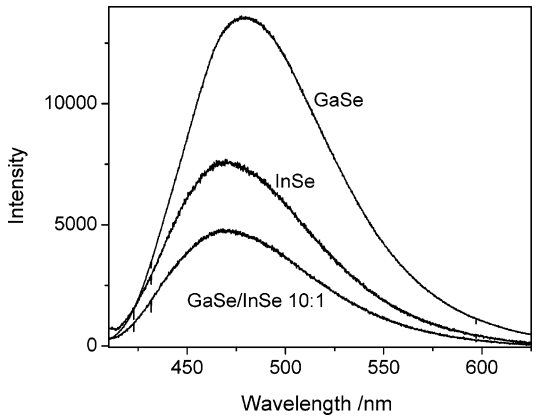

Figure 2. Static fluorescence spectra of GaSe nanoparticles, InSe nanoparticles, and GaSe/InSe mixture in equilibrium. The intensities are normalized to the corresponding amount of 387.5 nm light absorbed.

equilibrium in approximately 1 day. This is the same time scale on which aggregates form when a volatile solvent (such as pentane) is pumped off of a dilute, monomer solution. We infer that this is also the time needed for InSe particles to intercalate into the GaSe aggregates. At equilibrium, the spectrum develops an additional absorption having an onset at ~396 nm, 3.13 eV. This observation indicates the presence of specific interactions between the two types of nanoparticles. This is reminiscent of the behavior previously seen in InSe/GaSe (10:1) mixed aggregates.[11] However, those studies used much smaller GaSe particles and therefore very different energetics. They also had an opposite InSe/GaSe ratio. In light of these considerations, there is no a priori reason to expect that the assignment of the absorption feature seen here will be the same as that observed in the previous studies. (Below, we will show that the assignments are not the same.) Assignment of this spectral feature and elucidation of the exciton dynamics in the mixed aggregates are facilitated by static emission, transient absorption, and time-resolved emission results. We note that the time-resolved absorption studies are performed with 387.5 nm excitation light. At this wavelength both the new GaSe/InSe heterojunction feature and the lowest-energy GaSe absorption are excited. Comparison of the absorption spectrum immediately after mixing and at equilibrium indicated that the 387.5 nm absorbance increases by approximately one-third (Figure 1). Thus, approximately one-fourth of the excitation is into the heterojunction absorption with the remaining three-fourths into the GaSe particles. Assignment of the new transition is based on the idea that these two overlapping absorptions correspond to excitation into different parts of the aggregate and will result in different excited-state behavior.

The static fluorescence spectra of GaSe particles, InSe particles, and the GaSe/InSe mixture are shown in Figure 2. The fluorescence spectrum and excitation-dependent quantum yields of the GaSe particles are very similar to those reported in previous papers.[9,16,17] They are moderately emissive, with a quantum yield of ~9%, following 387.5 nm excitation. The InSe particles are less emissive with a quantum yield ~5%. It was previously reported[2] that the small (2.9 nm) InSe particles exhibit high quantum yield, ~12−25%, while midsized particles (4.6 nm) exhibit very small quantum yield ~0.5%. The lower quantum yield in the present case may reflect a larger number of midsized particles in this sample. The GaSe/InSe mixture has a low fluorescence quantum yield, approximately 3%. These results and fluorescence excitation spectra suggest that excitation of the GaSe/InSe heterojunction feature results in little or no fluorescence and that there are additional quenching mechanisms following excitation of the GaSe absorption. The time-resolved absorption and fluorescence results presented below facilitate assignment of the GaSe/InSe heterojunction absorption and elucidation of the additional fluorescence quenching mechanisms.

Transient absorption (TA) difference spectra (absorbance following excitation minus absorbance without excitation) of the equilibrium GaSe/InSe are shown in Figure 3. The TA spectra of GaSe particles and InSe particles are also presented in Figure 3. Figure 3A shows that at times less than 20 ps the mixture TA spectrum is similar to that of the InSe particles. Specifically there is considerable absorption in the blue, and the zero crossing is at ~500 nm. At longer times (200 ps), the relative amount of absorption in the blue decreases, and the zero crossing moves to 530 nm. These long time TA spectra are similar to those of the GaSe particles. It is also of interest to note the transient absorption kinetics obtained at 650 nm (Figure 3B). The kinetics show a biphasic decay, consisting of 19 and 300 ps components. In comparison, the GaSe TA kinetics show no fast decay component (Figure 3C). This is consistent with previous results on large GaSe nanoparticles; photoexcitation produces an electron−hole pair at Γ that slowly relaxes by carrier trapping.[7] There are no fast electron or hole relaxation processes in these particles. In contrast, the InSe nanoparticles show a significant decay within the first 50 ps (Figure 3D). This is consistent with previously reported results on InSe nanoparticles that show a significant 15 ps decay component. In the InSe case, the electron exhibits a strong intraband absorption at Γ but not at M, and the fast decay component is assigned to $\Gamma \rightarrow M$ momentum relaxation.[8] It is important to note that in the case of large GaSe and all but the smallest InSe nanoparticles the only process that gives rise to a fast decay component in the TA results is electron relaxation in the InSe conduction band. In the present GaSe/InSe sample, InSe particles account for approximately 10% of the absorption. At this concentration, InSe nanoparticles by themselves give only a very weak TA spectrum. Thus, the observed decay cannot come from decay of InSe particles following direct band gap excitation. These results clearly indicate that excitation of the heterojunction band in the mixture spectrum results in dynamics that are absent in either type of particle alone. The long time spectra are similar to those of GaSe, and the large particle GaSe TA spectra are dominated by a hole intraband transition.[7] This indicates that the holes are in the GaSe valence band. However, the fast decay component indicates that the electrons are, at least initially, in the InSe conduction band. Taken together, these observations indicate that photoexcitation of the heterojunction band in the mixed aggregates is a charge-transfer band and results in direct GaSe to InSe electron transfer. This is followed by electron momentum relaxation in the InSe conduction band on the 20 ps time scale. We also note that the amplitude of the fast decay is quite large, more than one-third of the total. This implies that some fraction of excitation that is nominally to the GaSe conduction band also results in an electron in the InSe conduction band within a few picoseconds. This is presumably from excitation of GaSe particles adjacent to InSe particles in the aggregate. It is an important observation because it indicates that an exciton on a GaSe particle undergoes rapid electron transfer to an adjacent InSe particle and therefore quenches. Because these aggregates are 90% GaSe particles, exciton quenching at a heterojunction provides an experimental probe of the GaSe exciton dynamics.

Exciton Diffusion/Quenching Dynamics. As stated above, approximately three-fourths of the 387.5 nm excitation is to the

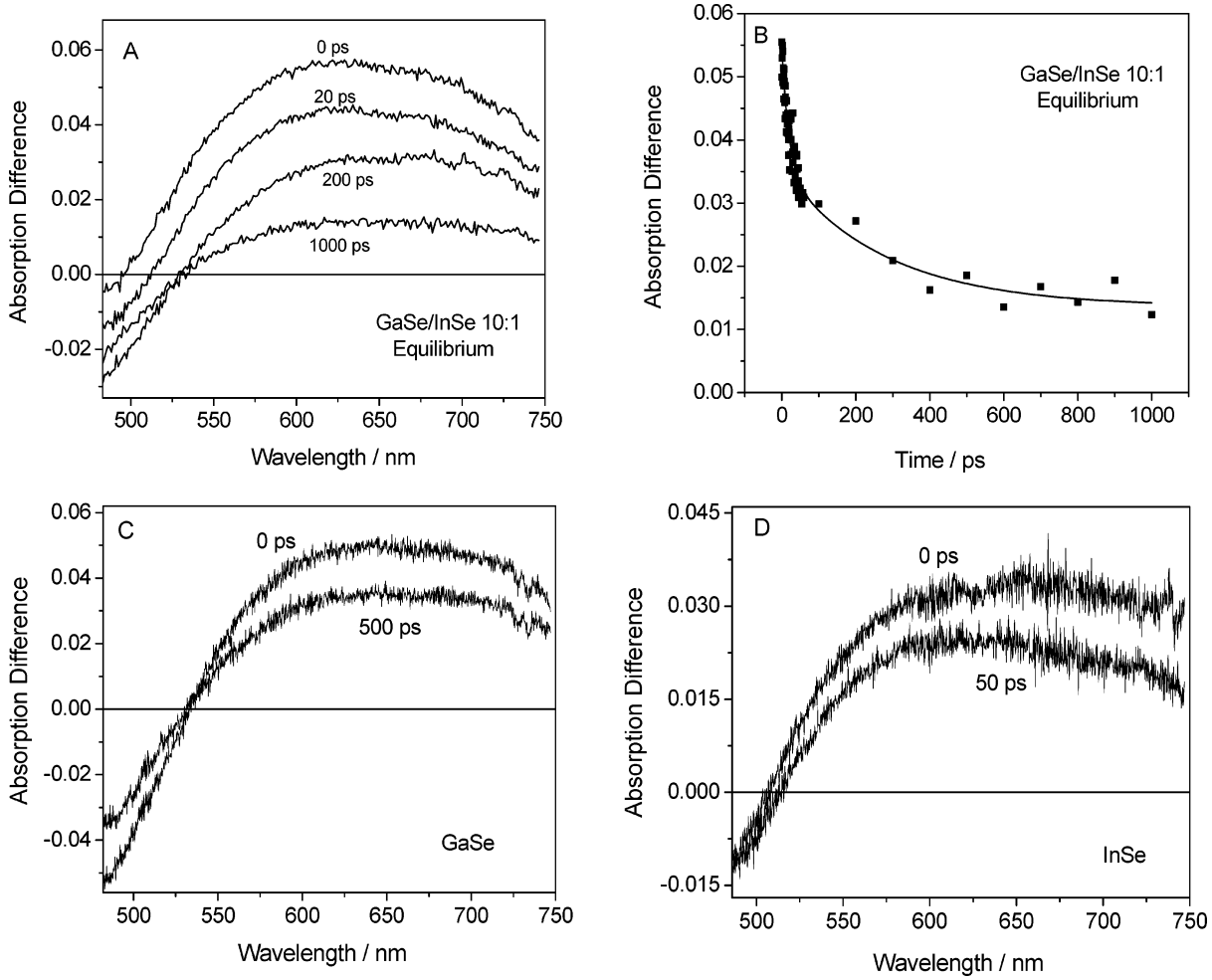

Figure 3. (A) Transient absorption spectra of GaSe/InSe mixture in equilibrium at 0, 20, 200, and 1000 ps. (B) Transient absorption kinetics of GaSe/InSe mixture in equilibrium at 650 nm. (C) Transient absorption spectra of GaSe nanoparticles at 0 and 500 ps. (D) Transient absorption spectra of InSe nanoparticles at 0 and 50 ps.

GaSe band gap excitons. These excitons can undergo diffusion along the one-dimensional aggregates, and the diffusion rates in GaSe aggregates have been studied in a previous paper.[10] If the exciton diffuses to a GaSe/InSe heterojunction, then we expect it will undergo charge separation, just as occurs following direct excitation of the heterojunction charge-transfer band. The charge-separated state is nonfluorescent, and this will result in fluorescence quenching. Thus in these mixed aggregates, it is possible to elucidate the exciton diffusion and charge separation dynamics using time-resolved fluorescence spectroscopy. The fluorescence decay kinetics for the GaSe aggregates and GaSe/InSe mixed aggregates are shown in Figure 4. The GaSe kinetics are fit with a biexponential decay having 1.05 ns (45%) and 3.7 ns (55%) components. The faster decay of the mixed aggregates is indicative of the rates of exciton diffusion and subsequent quenching. The static absorption spectra along with these measurements allow us to understand the lower fluorescence quantum yield of the mixed aggregates. Three factors contribute to increased quenching in the mixed aggregates: First, some fraction of the excitation is absorbed by the charge-transfer band, second, some of the GaSe particles are adjacent to InSe particles and therefore are immediately quenched, and finally, diffusive quenching also contributes. The quantitative effects of each of these factors are easily evaluated. The fraction of the 387.5 nm light that goes into to the GaSe localized absorption (rather than the nonfluorescent charge-transfer band) is approximately 75%. In a random mixed aggregate having a GaSe to InSe ratio of 10:1, the fraction of absorbing nanoparticles that are not InSe or GaSe particles adjacent to InSe particles is 73%. Finally, the ratio of the areas under the fluorescence decay curves when normalized at $t = 0$ is 0.74. (That these factors are approximately the same is a coincidence. They vary with excitation wavelength and concentration ratio.) The product of these factors is 0.40, and the ratio of the fluorescence quantum yields is predicted to be this value. With a GaSe aggregate quantum yield of 9.0%, this predicts a mixed

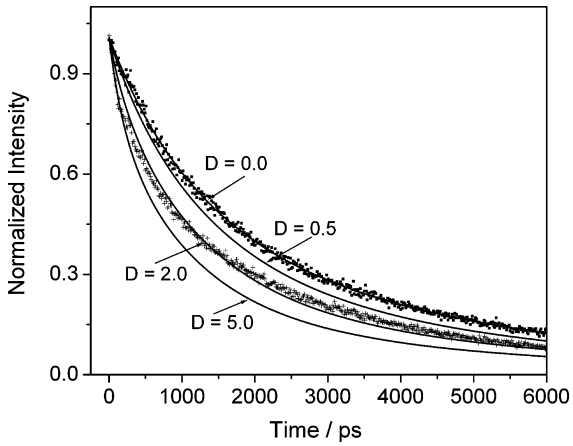

Figure 4. Fluorescence decay kinetics for GaSe aggregates (solid dots) and GaSe/InSe mixed aggregates (pluses). The calculated fluorescence decay kinetics with diffusion coefficients of 0.0, 0.5, 2.0, and 5.0 nm^2/ns are also shown.

aggregate quantum yield of 3.6%, in agreement with the measured value of 3.2%.

The diffusive quenching dynamics can be semiquantitatively understood in terms of simple fits to the fluorescence decay curves and a back-of-the-envelope calculation, as follows. The GaSe aggregate and GaSe/InSe fluorescence decay curves can be fit to biexponential decays. In the case of the GaSe aggregates, the fast component is 1.05 ns and is assigned to hole trapping. The mixed aggregate decay is fit with a fast component of 610 ps. Since hole trapping and exciton quenching at a heterojunction concurrently quench the fluorescence, the net decay time is given by $1/\tau_{hj} = 1/\tau_{trap} + 1/\tau_{diff}$, where τ_{trap} is the hole trapping time (1.05 ns), τ_{hj} is the observed decay time for the mixed aggregates (~610 ps), and τ_{diff} is the average time required for the exciton to diffuse to a heterojunction. This gives an exciton diffusion time of ~1.4 ns. If an average diffusion distance can be estimated, then a value of the one-dimensional diffusion coefficient, D, can then be obtained from the Einstein−Smoluchowski equation: $D = |\langle x \rangle|^2/2\tau_{diff}$. The average distance that an exciton has to go in a specific direction along the aggregate to find a heterojunction in a 10:1 random GaSe/InSe mixed aggregate is on the order of 4 particles. (Recall that quenching occurs when the exciton reaches the GaSe particle next to an InSe particle; hence the average distance is 4 rather than 5 particles.) However, the exciton can diffuse in either direction, and the nearest heterojunction will usually be closer than 4 particles. The estimate of 4 particles is therefore an upper limit, and the value of the diffusion coefficient estimated in this way is likely to be the correct order-of-magnitude but a bit high. If $\langle x \rangle$ is taken to be 4 particles (~3.2 nm), then this approximate calculation gives a diffusion constant of ~5−6 (particle separations)^2/ns or ~3.5 nm^2/ns. This is somewhat (75%) higher than the value of 2 nm^2/ns obtained from dilution-dependent anisotropy decay studies previously published.[10]

The diffusion dynamics also can be modeled quantitatively, and an exciton diffusion coefficient can be extracted from the experimental fluorescence decay curves using the following Monte Carlo procedure. It is assumed that the GaSe and InSe particles occur randomly in the mixed aggregate. The particle to be excited is then selected at random, and this initiates a trajectory. If the excited particle is an InSe or next to an InSe, then the emission is assumed to be immediately quenched and that is the end of that diffusive trajectory. If not, then the selected particle can fluoresce or diffuse, i.e., jump to an adjacent particle. The probability of fluorescence in the specified time interval is determined by the observed GaSe fluorescence decay curve. Similarly, the probability of jumping to an adjacent particle is given by the diffusion coefficient. If after a jump the newly excited particle is next to an InSe, then that diffusive trajectory is ended. Many trajectories are run, and a fluorescence histogram is built up. It was reported previously that the diffusion coefficient of GaSe nanoparticles is ~2 nm^2/ns.[10] The results of the simulation using this value for the diffusion coefficient are shown in Figure 4. Calculated curves corresponding to diffusion coefficients of 0.50 and 5.0 nm^2/ns are also shown for comparison. It is important to note that once the diffusion coefficient is specified this is a zero adjustable parameter fit. As shown in Figure 4, the calculated and the experimental curves match very well. In the previous studies, the exciton diffusion coefficients were determined from concentration-dependent fluorescence anisotropy decays in GaSe (no InSe) aggregates.[10] Thus, exciton diffusion coefficients determined in completely different ways agree within the experimental uncertainty. This gives a detailed picture of the diffusion mechanism resulting in charge separation in the nanoparticle heterojunction.

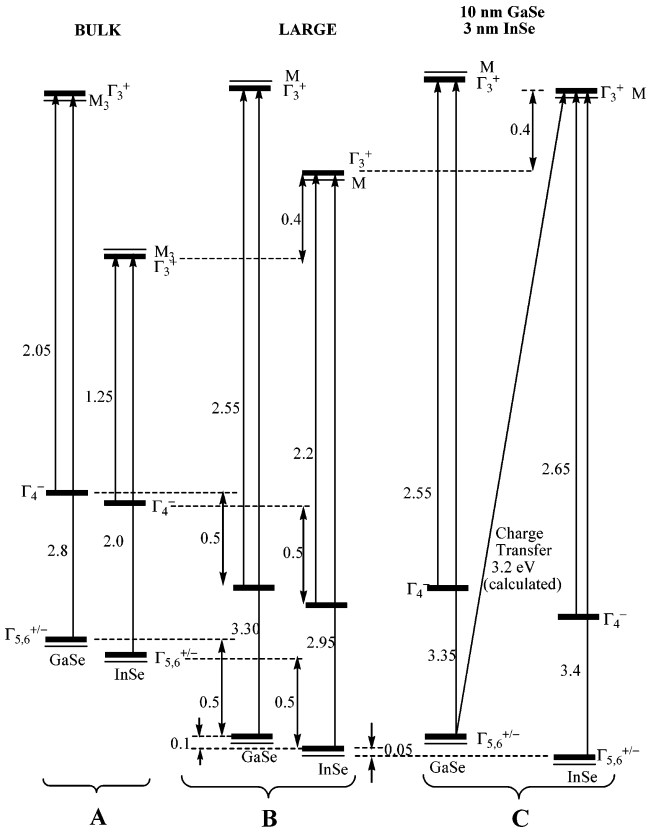

Figure 5. Schematic energy diagram of (A) a bulk GaSe/InSe heterojunction, the energetics of large, (B) two-dimensional GaSe and InSe particles (z quantum confinement only), and (C) the GaSe/InSe nanoparticle heterojunction studied here. Optical transitions are shown with single-headed arrows, and some of the other energy gaps are indicated with double-headed arrows. Levels involving optically allowed transitions are shown with heavy lines.

Heterojunction Energetics. The energy diagram of GaSe/InSe nanoparticle heterojunctions can be calculated from the energy diagram of bulk thin film GaSe/InSe heterojunctions and quantum confinement energies. The energetics of the charge-transfer bands are obtained from this diagram and may be compared to those inferred from the observed spectra. The band gaps ($\Gamma_3^+ - \Gamma_4^-$) of GaSe and InSe are 2.05 and 1.25 eV, respectively.[12,18−20] Photoelectron spectra indicate that in bulk thin film heterojunctions the conduction band offset, Γ_3^+(GaSe)−Γ_3^+(InSe), is 0.9 eV and the valence band offset, Γ_4^-(GaSe)−Γ_4^-(InSe), is 0.1 eV.[12] These offsets are shown in Figure 5A. Quantum confinement shifts both the conduction and the valence band energies. GaSe and InSe particles show different amounts of z-axis quantum confinement, but because all of the particles have the same thickness (they are all single tetralayers), the extent of z-axis quantum confinement is size-independent. The extents of z-axis quantum confinement are derived from optical measurements on nanoparticles[2,7,13] and are approximately 0.50 and 0.93 eV, for GaSe and InSe particles, respectively. These values are and are consistent with the band structure calculations.[6] The large-particle energetics (considering only z-axis quantum confinement) are shown in Figure 5B. Size-dependent conduction and valence band xy quantum confinement also occurs in both InSe and GaSe particles.[2,7] The nanoparticles used in these experiments have $\Gamma_3^+ - \Gamma_4^-$ band gaps of 2.64 and 2.68 eV for GaSe and InSe, respectively. Thus, the total (z-axis plus xy-plane) quantum confinement energies are

~0.6 eV for the GaSe nanoparticles and ~1.4 eV for the InSe nanoparticles. Most of the *xy* quantum confinement is in the conduction band, and the ratio of valence and conduction band *xy* quantum confinement energies is taken as the ratio of hole and electron effective masses.[4,21,22] The 3 nm InSe particles exhibit considerable (~0.5 eV) *xy* quantum confinement. In contrast, the 10 nm GaSe particles are sufficiently large that they exhibit very little *xy* quantum confinement. The higher-energy *xy*-polarized absorption is assigned to a Γ_6^- to Γ_3^+ transition, and the $\Gamma_3^+ - \Gamma_6^{+/-}$ energy differences may also be obtained from the static absorption spectra. The InSe particles exhibit a shift of ~0.50 eV from quantum confinement in the *xy*-plane. These energies are more difficult to estimate accurately, because the spectroscopy of the $\Gamma_6^- \rightarrow \Gamma_3^+$ transition is very sensitive to particle aggregation. However, values of appoximately 3.38 and 3.30 eV can be estimated for the present GaSe and InSe nanoparticles, respectively, and are also consistent with the band structure calculations. The energetics in the present case (10 nm GaSe, 3 nm InSe) are derived from these considerations and shown in Figure 5C. These simple considerations lead to the prediction that the GaSe to InSe charge transfer occurs at 3.2 eV. This is essentially quantitative agreement with the observed charge-transfer onset at 396 nm, 3.13 eV.

Figure 5 shows that the GaSe and InSe conduction bands are close to the same energy. We suggest the intensity of the charge-transfer band depends on the extent of mixing of the Γ_3^- conduction band levels. The extent of mixing between wave functions on different particles depends on the energy differences and the overlaps. Without such mixing, the states on different nanoparticles are orthogonal, and any interparticle transition has zero oscillator strength. The energetic proximity depends on quantum confinement effects, and the combination of large GaSe and small InSe results in near resonance of the conduction bands. Furthermore, significant overlap is expected between the Γ_3^- conduction band orbitals. The extent of overlap depends on the spatial characteristics of the orbitals and can be qualitatively assessed from band structure calculations. If the orbitals extend out of the tetralayer sheets, then there will be a significant interlayer splitting in the bulk material, and spatially confined orbitals will exhibit very little splitting. Specifically, states that can exhibit large coupling to adjacent particles and are degenerate at the A-point will have large splitting at Γ. This is the case for the Γ_3^+/Γ_2^- pair at the bottom of the conduction band, especially for InSe.[3,6] These levels exhibit large interlayer splittings, comparing the energies at the A- and Γ-points. This is also apparent from elementary considerations of the atomic orbitals involved in these states; the Γ_3^+ levels have large selenium s* and gallium p_z contributions.[3,6] Both considerations indicate that significant overlap and hence mixing of the conduction band levels would be expected. Thus, Figure 5 provides only a zeroth order picture of the states involved in the charge transfer; the acceptor state is actually a mixed InSe/GaSe Γ_3^+ level. We note that this is not the case for the $\Gamma_5^{+/-}$ and $\Gamma_6^{+/-}$ valence band levels. The $\Gamma_5^{+/-}$ and $\Gamma_6^{+/-}$ orbitals exhibit very small interlayer splittings and are primarily involved in Ga−Se bonding. Both considerations indicate that these orbitals are largely confined to the interior of the nanoparticle and should exhibit very little mixing. We conclude that energetic proximity of the conduction band levels is needed for there to be an intense charge-transfer band in these heterojunctions.

In a previous study spectroscopic and dynamic results were reported that indicated the presence of an InSe to GaSe charge-transfer band—the opposite of what is observed here.[11] These studies used comparable or slightly smaller InSe particles and much smaller (2.7 nm) GaSe particles in an GaSe/InSe ratio of 1:10. It is also possible to analyze the energetics in the previous study of InSe/GaSe heterojunctions in terms of these energetics and quantum confinement considerations. The most obvious difference is that the previous, much smaller GaSe particles exhibit far more quantum confinement than those used in the present study. As a result, the small-particle GaSe Γ_3^+ conduction band level is expected to be considerably higher in energy (~0.5 eV) than that in the present case (Figure 5). In this case, the InSe to GaSe charge-transfer band would be expected at a higher energy than the InSe Γ_6^- to Γ_3^+ transition, contrary to what was observed. Thus, the simple model in Figure 5 fails to explain the energetics observed in the previous study. The reason for this discrepancy is at this point unclear. There are two obvious possibilities. First, the model in Figure 5 fails to take aggregation effects into account. Aggregation can shift the observed transitions by thousands of wavenumbers and therefore could alter the total energetic picture. Second, the presence of strongly coordinating, electron donating or electron accepting ligands could alter the redox characteristics and charge-transfer spectroscopy of the particles. In the present study, the nanoparticles were dissolved in a highly purified, weakly coordinating solvent mixture. The solvent is mostly octane, approximately 10% TOP, and a very small amount of TOPO. In contrast, the previous studies used much higher TOP and especially TOPO concentrations. Furthermore, those reagents were not as thoroughly purified as in the present case. (For example, the TOP was purified by a single vacuum distillation.) As a result, small quantities of very strongly binding ligands, such as phosphonates, could also be present in those samples. This could result in differential stabilization and electron donation to the InSe and GaSe nanoparticles, thereby complicating the charge-transfer energetics. A systematic study of the factors controlling the energetics of these heterojunctions is currently underway and will be reported in a later paper.

Conclusions

Several conclusions can be drawn from the results presented here:

1. GaSe/InSe mixed aggregates spontaneously form at high concentrations in nonpolar solvents and exhibit an intense new band in the absorption spectrum.

2. The heterojunction absorption is assigned based on a combination of static and time-resolved absorption spectra. The assignment is to a GaSe $\Gamma_5^{+/-}$ or $\Gamma_6^{+/-}$ to InSe Γ_3^+ charge-transfer transition.

3. Direct excitation to the GaSe part of the mixed aggregates results in an exciton that can undergo subsequent diffusion along the one-dimensional aggregate. Diffusion to a heterojunction results in fluorescence quenching. This process can be modeled, and an exciton diffusion coefficient can be extracted from the fluorescence decays. The calculated and experimental decay curves are in excellent agreement and yield the same diffusion coefficient as previously determined through concentration-dependent anisotropy decay measurements.

4. The nanoparticle valence and conduction band offset energetics may be calculated from published bulk InSe/GaSe heterojunction energetics and known quantum confinement energetics. The calculated energy of the GaSe to InSe charge-transfer band may then be compared to that inferred from the static absorption spectra. These energetics are in good agreement.

Acknowledgment. This work was supported by a grant from the U. S. Department of Energy (Grant No. DE-FG02-04ER15502).

References and Notes

(1) Chikan, V.; Kelley, D. F. *Nano Lett.* **2002**, *2*, 141.
(2) Yang, S.; Kelley, D. F. *J. Phys. Chem. B* **2005**, *109*, 12701.
(3) Schluter, M. *Nuovo Cimento Soc. Ital. Fis., B* **1973**, *13*, 313.
(4) Mooser, E.; Schluter, M. *Nuovo Cimento Soc. Ital. Fis., B* **1973**, *18*, 164.
(5) Doni, E.; Girlanda, R.; Grasso, V.; Balzarotti, A.; Piacentini, M. *Nuovo Cimento Soc. Ital. Fis., B* **1979**, *51*, 154.
(6) Camara, M. O. D.; Mauger, A.; Devos, I. *Phys. Rev. B* **2002**, *65*, 125206.
(7) Tu, H.; Mogyorosi, K.; Kelley, D. F. *Phys. Rev. B* **2005**, *72*, 205306.
(8) Yang, S.; Kelley, D. F. *J. Phys. Chem. B* **2006**, *110*, 13430.
(9) Tu, H.; Yang, S.; Chikan, V.; Kelley, D. F. *J. Phys. Chem. B* **2004**, *108*, 4701.
(10) Tu, H.; Mogyorosi, K.; Kelley, D. F. *J. Chem. Phys.* **2005**, *122*, 44709.
(11) Tu, H.; Kelley, D. F. *Nano Lett.* **2006**, *6*, 116.
(12) Lang, O.; Klein, A.; Pettenkofer, C.; Jaegermann, W.; Chevy, A. *J. Appl. Phys.* **1996**, *80*, 3817.
(13) Tu, H.; Chikan, V.; Kelley, D. F. *J. Phys. Chem. B* **2003**, *107*, 10389.
(14) Brus, L. E. *J. Chem. Phys.* **1984**, *80*, 4403.
(15) Leatherdale, C. A.; Woo, W.-K.; Mikulec, F. V.; Bawendi, M. G. *J. Phys. Chem. B* **2002**, *106*, 7619.
(16) Chikan, V.; Kelley, D. F. *Nano Lett.* **2002**, *2*, 1015.
(17) Chikan, V.; Kelley, D. F. *J. Chem. Phys.* **2002**, *117*, 8944.
(18) Piacentini, M.; Doni, E.; Girlanda, R.; Grasso, V.; Balzarotti, A. *Nuovo Cimento Soc. Ital. Fis., B* **1979**, *54*, 269.
(19) Manjón, F. J.; Errandonea, D.; Segura, A.; Muñoz, V.; Tobías, G.; Ordejón; Canadell, E. *Phys. Rev. B* **2001**, *63*, 125330.
(20) Emery, J.-Y.; Brahim-Ostmane, L.; Hirlimann, C.; Chevy, A. *J. Appl. Phys.* **1992**, *71*, 3256.
(21) Kress-Rogers, E.; Nicholas, R. J.; Portal, J. C.; Chevy, A. *Solid State Commun.* **1982**, *44*, 379.
(22) Ottaviani, G.; Canali, C.; Nava, F.; Schmid, P.; Mooser, E.; Minder, R.; Zschokke, I. *Solid State Commun.* **1974**, *14*, 933.